Thermal expansion measurements and the phase transition in the compound $GdSi_2$

2004 J. Phys.: Condens. Matter 16 7787

(http://iopscience.iop.org/0953-8984/16/43/018)

INSTITUTE OF PHYSICS PUBLISHING JOURNAL OF PHYSICS: CONDENSED MATTER

J. Phys.: Condens. Matter **16** (2004) 7787–7792 PII: S0953-8984(04)83591-4

Thermal expansion measurements and the phase transition in the compound $GdSi_2$

F X Zhang, P Limermann, Hexiong Yang and S K Saxena

CeSMEC, Florida International University, University Park, Miami, FL 33199, USA

Received 14 July 2004, in final form 21 September 2004
Published 15 October 2004
Online at stacks.iop.org/JPhysCM/16/7787
doi:10.1088/0953-8984/16/43/018

Abstract

The temperature dependence of the structural parameters of orthorhombic silicide $GdSi_2$ was studied by the *in situ* powder x-ray diffraction method. A structural change from orthorhombic to α-$ThSi_2$-type tetragonal was found at around 818 K. The change in structure with temperature is continuous and reversible without a discontinuous change in volume. The thermal expansion coefficient was calculated from the refined cell parameters. The compound began to react with the residual oxygen in the argon environment and form oxide above 973 K.

(Some figures in this article are in colour only in the electronic version)

1. Introduction

Rare-earth silicides have attracted considerable attention in the past few decades because of the wide potential field of applications. Rare-earth silicides can be epitaxially grown on n-type Si substrate to form systems with the lowest known Schottky barrier heights (∼0.3–0.4 eV), suggesting application in infrared detectors [1–3]. Some rare-earth silicides also have many interesting electron transport and magnetism-related properties, such as an unusual giant magnetocaloric effect [4], a giant magnetoresistance effect [5] and colossal magnetostriction [6] in the compounds $Gd_5(Si_{1-x}Ge_x)_4$ and superconductivity in $LaSi_2$ [7]. There are two basic structure types for rare-earth disilicides. The late 4f rare-earth metal disilicides, after Gd, usually form an AlB_2-type structure in which the silicon atoms are arranged in coplanar hexagonal nets like in graphite and the metal atom layer is sandwiched between the silicon layers [8]. The early 4f rare-earth metal disilicides usually have the α-$ThSi_2$ structure [9], in which planar three-dimensional silicon groups are connected with each other by twisting alternately by 90° so as to form a tetragonal three-dimensional open network (figure 1); the metal atoms are placed in the interstices and bonded to 12 Si neighbours. The Si atoms in $GdSi_2$ form a three-dimensional open network similar to that in α-$ThSi_2$, but $GdSi_2$ shows an orthorhombic symmetry with only little difference [10] for the cell parameters a and b. During film processing, another silicon vacancy defect, disilicide (with the composition of

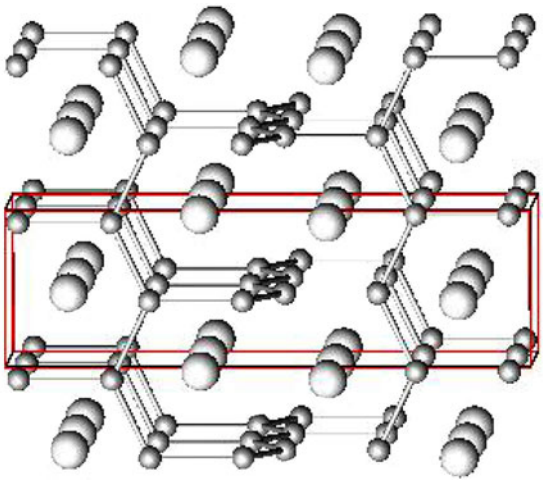

Figure 1. A schematic diagram of the orthorhombic and tetragonal α-$ThSi_2$-type structures for $GdSi_2$. The big atoms are Gd. The smaller Si atoms in orthorhombic $GdSi_2$ have two nonequivalent 4e sites along the a and b directions.

$GdSi_{1.7}$), which has the AlB_2-type form, always coexists with the orthorhombic $GdSi_2$ [11, 12]. For the synthesis and potential application of gadolinium silicides, structure stability at high temperature is also important. In this paper, we have measured the temperature dependence of the structure parameters of $GdSi_2$; orthorhombic $GdSi_2$ was found to transform completely to the normal α-$ThSi_2$-type tetragonal phase at temperatures above 818 K. The volume temperature coefficient and structure stability are also studied.

2. Experimental methods

The $GdSi_2$ is a commercial product (Alfa-Aesar Chem.) with purity above 99.9%. The sample is heated by a resistance method with a graphite heater and protected in a flowing argon atmosphere during the experiments. The sample is inserted in a hole ($\varnothing \sim 1.5$ mm), which is located at the centre of the graphite plate. In order to measure the temperature, a PtRh (13%)/Pt thermocouple is used. The junction tip of the thermal couple is directly buried in the sample powder and the temperature deviation is below 2 K. The *in situ* x-ray diffraction measurements were performed on a Bruker micro-x-ray system using the Kα radiation from a rotating Mo target. The Bragg diffraction rings were first recorded with a smart CCD system and the then integrated into two-dimensional patterns by Bruker software. Between runs, there was 5–10 min interval to allow the sample to reach to an equilibrium temperature. The XRD patterns were analysed with Rietveld refinement so as to derive the detailed structure parameters by using the program FULLPROF [13] after subtracting the background.

3. Results and discussion

The structure of $GdSi_2$ at room temperature is of orthorhombic symmetry (space group $Imma$ (No 74), $a = 4.0098$ Å, $b = 4.0885$ Å and $c = 13.4359$ Å). Figure 2 shows the refinement results for the XRD pattern taken at room temperature. Due to the difference between the lattice parameters a and b, the (200) and (020) Bragg peaks at $\sim 20°$ in the pattern are clearly separated. The positions of the two peaks become closer with increase of the temperature. Figure 3 shows the evolution of the two peaks with temperature. At 818 K, the two peaks overlapped completely, which means that the parameters a and b became equal and the structure had changed from orthorhombic to tetragonal. The above change of lattice parameters is continuous and the tetragonal phase should have the same structure for all early rare-earth

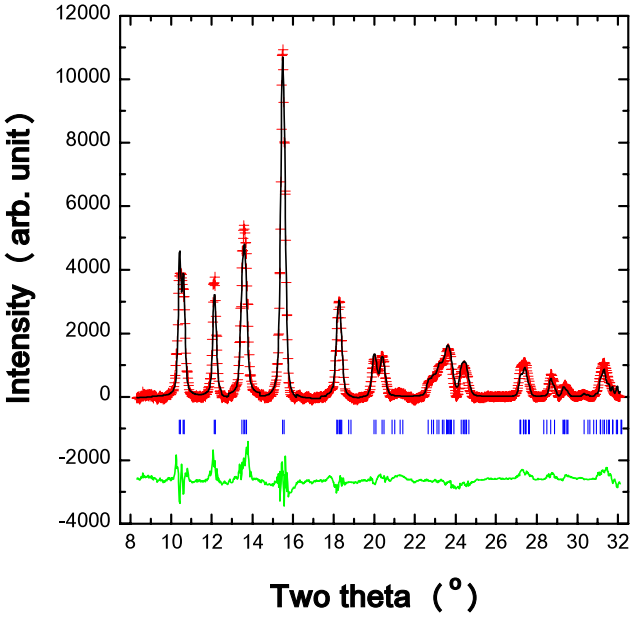

Figure 2. Rietveld refinement of the XRD pattern taken at room temperature. The structure is of orthorhombic symmetry with space group *Imma* and cell parameters of $a = 4.0098$ Å, $b = 4.0885$ Å, $c = 13.4359$ Å; fitting results: $R_p = 2.92\%$, $R_{wp} = 4.02$, $\chi^2 = 6.56$.

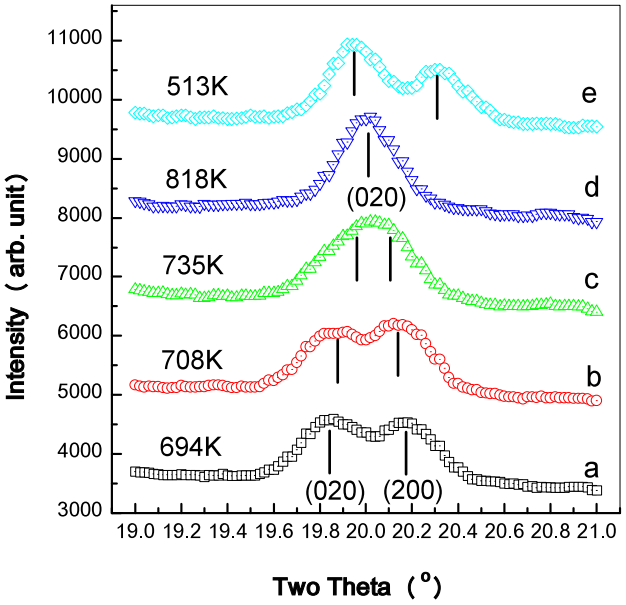

Figure 3. The XRD patterns around 20° taken before and after the phase transition. The two (020) and (200) Bragg peaks for the orthorhombic $GdSi_2$ changed to one peak—(020)—for the tetragonal structure at 818 K (patterns (a)–(d)) and this changes back to two peaks when the temperature is reduced (e).

disilicides. It has the α-$ThSi_2$ structure type with the space group of $I4_1/amd$ (No 141). The XRD patterns taken at 818 K, calculated with the tetragonal space group $I4_1/amd$, are plotted in figure 4 and they fit quite well. In order to get the temperature dependence of the structure parameters, all the XRD patterns taken at different temperatures were refined with the least squares method by the program FULLPROF, with the orthorhombic space group *Imma* for those taken below 818 K and the tetragonal space group $I4_1/amd$ for those taken above 818 K. The temperature dependence of the refined lattice parameters and cell volume is plotted in figure 5. The lattice parameters a and b increase with temperature at the beginning. But they

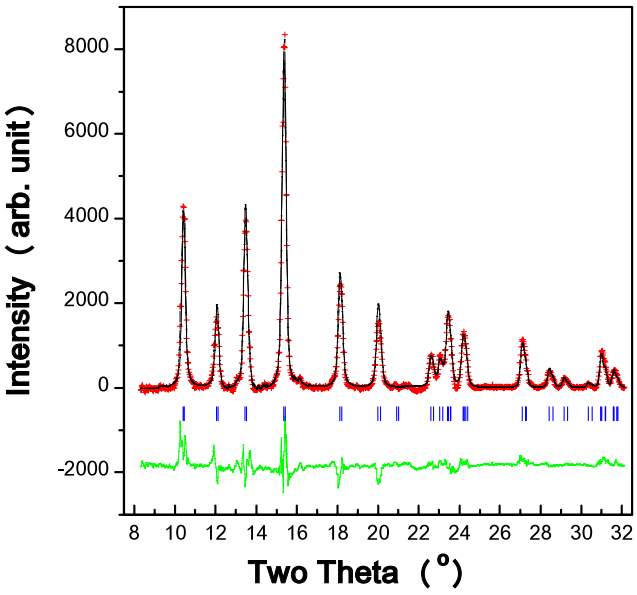

Figure 4. The Rietveld refinement of the XRD pattern taken at 818 K. The structure is of tetragonal symmetry with space group $I4_1/amd$ and cell parameters of $a = b = 4.08529$ Å, $c = 13.5092$ Å; fitting results: $R_p = 1.90\%$, $R_{wp} = 2.71$, $\chi^2 = 2.96$.

show different behaviours after 680 K—parameter a continues to increase with a larger slope, while parameter b decreases with temperature. At 818 K, a and b reach the same value and the structure of $GdSi_2$ changes from orthorhombic to tetragonal. The temperature dependence of the c parameter also has a distinct slope change at 680 K. However, the change of cell volume has no discontinuity over the whole temperature range (figure 5(c)) and the orthorhombic to tetragonal change in $GdSi_2$ is thus a second-order phase transition. The XRD patterns between 680 and 818 K can be indexed with the orthorhombic unit cell, but we believe that the orthorhombic to tetragonal phase transition should begin at 680 K and finish at 818 K. Our experimental results also indicate that the above orthorhombic to tetragonal phase transition is reversible. In figure 3, when the temperature reduced from 980 K to 513 K, the (020) diffraction peak in the tetragonal phase separated into two peaks again.

In order to get the linear thermal expansion coefficient, we divided the curves in figures 5(a)–(c) into three parts—room temperature to 680 K, 680–818 K and 818–980 K, due to the distinct slope changes at 680 and 818 K. Each part is fitted with a third-order polynomial and the linear and volume thermal expansion coefficients κ and α are calculated with the following equations [14]:

$$k = \frac{1}{l}\frac{\partial l}{\partial T} \tag{1}$$

$$\alpha = \frac{1}{V}\frac{\partial V}{\partial T}. \tag{2}$$

The calculated linear thermal coefficients along the (100), (010) and (001) directions are shown in figures 6(a) and (b), respectively. They all show discontinuity at 680 and 818 K. The change of cell volume for $GdSi_2$ is continuous during the structural change and the V–T curve is fitted with a third order polynomial over the whole temperature range. The calculated volume thermal expansion coefficient is plotted in figure 6(c).

The Si–Si bonding length along the c axis has no obvious change in the orthorhombic phase and it increases with increase of temperature in the tetragonal phase; the bond becomes quite weak ($d > 2.35$ Å) above 873 K. The Si–Si bonding distance along the a direction

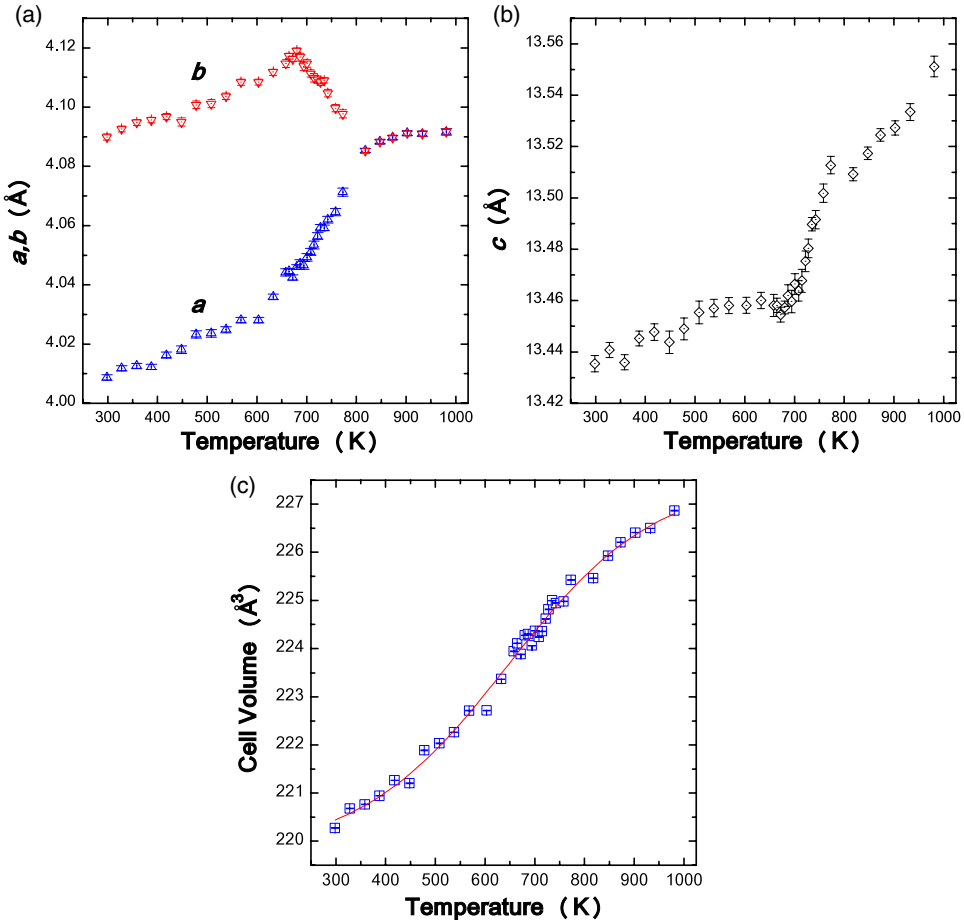

Figure 5. The temperature dependence of the cell parameters of $GdSi_2$. (a) *a* and *b*; (b) *c*; (c) cell volume. After 818 K, the structure is of tetragonal symmetry.

decreases slowly with temperature while the Si–Si bond along the *b* axis does not change significantly and reaches the same value in the final tetragonal phase. The Si–Si–Si bonding angles in the trends along the *a* or *b* directions show a slight change during heating and they reach the same value as in the tetragonal phase. Other Si–Si–Si bonding angles, which connect the two trends show no apparent change over the whole temperature range.

The Si in the $GdSi_2$ compound is not stable at higher temperatures even in the argon atmosphere. After 973 K, some of the Si has, in fact, reacted with the residual oxygen in the argon environment to form silicates, as seen from the XRD measurements. In our experiments, the Bragg peaks of $GdSi_2$ disappeared completely when the temperature was taken over 1373 K.

4. Conclusions

A structural change from orthorhombic (space group: *Imma*) to tetragonal (space group: $I4_1/amd$) was found by means of *in situ* XRD measurements for the compound $GdSi_2$ made while heating. The transition started at 680 K and was completed at around 818 K. The temperature-induced structural change is reversible. The linear and volume thermal expansion coefficients were calculated from the refined cell parameters.

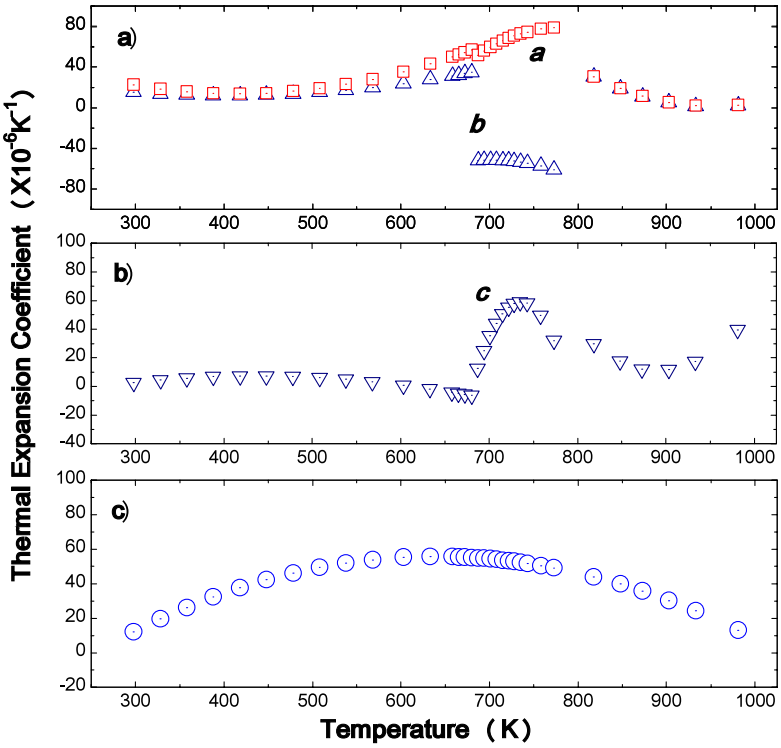

Figure 6. The temperature dependence of (a) the linear thermal expansion coefficient along the *a*, *b* directions; (b) the linear thermal expansion coefficient along the *c* direction; (c) the volume thermal expansion coefficient for $GdSi_2$.

Acknowledgments

This work was financially supported by the Division of Sponsored Research at FIU and grants from the National Science Foundation (DMR-0231291, EAR-00769641).

References

[1] Tu K U, Thompson R D and Tsaur B Y 1981 *Appl. Phys. Lett.* **38** 626
[2] Koleshko V M, Belisky V F and Knodin A A 1986 *Thin Solid Films* **141** 277
[3] Knapp J A and Picraux S T 1986 *Mater. Res. Soc. Symp. Proc.* **54** 261
[4] Pecharsky V K and Gschneidner K A Jr 1997 *Phys. Rev. Lett.* **78** 4494
[5] Pecharsky V K and Gschneidner K A Jr 2001 *Adv. Mater.* **13** 683
[6] Gschneidner K A, Pecharsky A O Jr, Pecharsky V K and Lograsso T A 2000 *Rare Earths and Actinides: Science Technology and Applications IV* (Warrendale, PA: Minerals, Metals and Materials Society)
[7] Henry W H, Betz C and Muir H 1962 *Bull. Am. Phys. Soc.* **7** 474
[8] Gladyshevskii E I 1979 *J. Less-Common Met.* **64** 213
[9] Nakano H and Yamanaka S 1994 *J. Solid State Chem.* **108** 260
[10] Perri J A, Binder I and Post B 1959 *J. Chem. Phys.* **63** 616
Perri J A, Binder I and Post B 1959 *J. Chem. Phys.* **63** 2073
[11] Chung K B, Choi Y K, Jang M H, Noh M and Whang C N 2003 *J. Appl. Phys.* **94** 212
[12] Molnár G, Gerös I, Petö G, Zsoldos E, Jároli E and Gyulai J 1988 *J. Appl. Phys.* **64** 6746
[13] Rodrguez-Carvajal J 2002 *FULLPROF—A Program for Rietveld Refinement* Version 2k (France: ILL)
[14] Pavlovic A S, Suresh Babu V and Seehra M S 1996 *J. Phys.: Condens. Matter* **8** 3139